On Heat Transfer within Gas Quenching Furnace

O. Macchion, S. Zahrai and J. W. Bouwman
Faxénlaboratoriet,
Royal Institute of Technology,
S-10044 Stockholm,
Sweden
http://www.faxenlaboratoriet.se/

Abstract: - Gas quenching in an industrial furnace is considered. The flow and thermal fields in the furnace with two different charges, plates and cylinders, in axial flow are studied numerically. Details of the thermal field characteristics are presented. A variation in heat transfer of maximum 125 % is observed in the whole basket, the maximum heat transfer being obtained on the first bodies of the charge. The heat transfer is found to be uniformly distributed in the middle of the charge, with mean values 50 % higher than on the sides. Recommendations for improvement of current vacuum quenching furnaces are proposed.

Key-Words: - Quench chamber; heat transfer uniformity; furnace design; hydrodynamic effects; axial flow.

1 Introduction

The industry of gas heat treating of metal pieces involves different operations, whose main types are austenitizing, homogenization, carburizing, and quenching. Quenching is the controlled rapid cooling of metals. Such regulated cooling of steel results in a controlled change of phase inside the metal improving its mechanical properties. As some examples, one may mention that quenching is used for hardening of parts such as gears, engine axles and bearing rings.

Gas quenching has a number of advantages in comparison with conventional methods. To start with, the quality of the surface is retained after that quenching is finalized. There is no need for post treatments, and there are no negative impacts on the environment as no harmful gases are used. It is also shown that the level of geometrical distortion is much lower, see e.g. Troell (1).

Gas quenching, as well as gas carburizing and other heat treating processes, occur in furnaces designed to sustain large pressures, typically between 5 to 20 bar. This constraint on the design leads to very complex flow paths, which in turn can lead to complex heat transfer fields. Thuvander et al (2) studied the gas quenching process and showed how heat transfer homogeneity influences the uniformity of the mechanical properties, in particular the hardness, of gas-quenched metal parts.

Despite the fact that the interaction between flow behavior and heat transfer is of crucial inportance for efficiency of the gas quenching process, very little is published on the subject. Bless and Edenhofer (3) and Pritchard et al (4) performed studies of gas quenching processes within gas quenching furnaces, but did not address the relation between design, flow pattern, and heat transfer within the working chamber. A study of the influence of the charge on the flow homogeneity upstream of the charge can be found in the work by Macchion et al (5). That study aimed at investigating the influence of the VUTK chamber design on the hydrodynamic properties of the fluid flow occuring in the chamber.

The main goal of the present work is to investigate the influence of the type of charge on the thermal field within gas quenching furnaces, as well as the relation between flow patterns and thermal effects within the working chamber and through the charge. The aim is to assess if the upstream good enough uniformity shown in the work by Macchion et al (5) is sufficient to ensure good enough quality of the heat treatment process.

The paper is organized as follows: first, the technical problem is presented in section 2. The mathematical model to be considered and the numerical procedure used for solving the resulting set of equations are outlined in section 3. The results are presented and analysed in section 4. section 5 sumarizes and concludes the work presented in this paper.

2 Problem statement

Achieving good enough uniformity of the heat transfer over the metal pieces to quench is a requirement when designing the working chamber of a quenching furnace. However it is often not sufficient to carefully design the quenching chamber entrance for such a purpose. The complexity of the heat transfer over the pieces arises both from the shape of the chamber and the non-uniform flow field around the metal pieces to quench.

This study focuses on the relation between flow patterns and heat transfer within the charge placed in the furnace whose model is presented in figure 1. This furnace model is the same as the one presented by Macchion et al (5). A complete description of the geometry and flow path is available in the work of Bless et al (3).

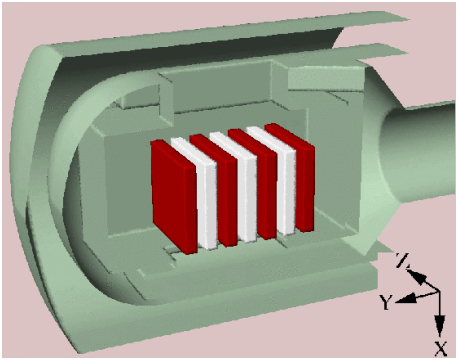

(a) Case with plates

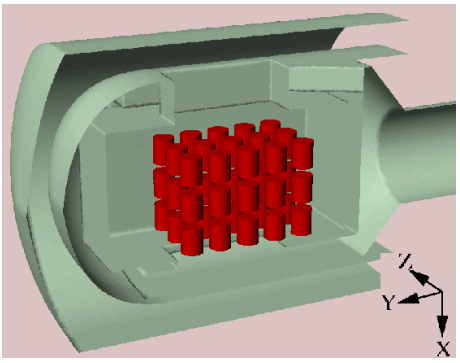

(b) Case with cylinders

Figure 1: Coordinates system used within the quenching chamber

Two different configurations are considered as examples of charge. The first configuration consists of 7 plates of dimensions 500 $\times$ 500 $\times$ 70 mm and in the second configuration, the VUTK furnace is charged with 45 cylinders, of length 150 mm and diameter 120 mm placed with their symmetry axis parallel to the main flow. These cylinders are at three horizontal planes with 5$\times$3 cylinders at each plane. See figure 1.

A coordinate system is defined in the following way. The axis Y is along the major axis and the axis Z along the minor axis. The main direction of the flow from the entrance box to the exit trap in denoted by X. Consequently, the plates are parallel to XZ plane with the center of the middle one coinciding with the origin of the coordinate system , i.e. $x = 0$, $y = 0$, and $z = 0$. The cylinders are placed at three different YZ planes with three cylindes in the direction of Y and five cylinders in the direction of Z. The center of the cylinder in the middle of the second plane coincides with the origin of the coordinate system.

The charge in the above configurations is assumed to be quenched in nitrogen at the reference pressure of 10 bar at a volume flow of 42000 m^3/h. This volume flow results in an inlet velocity of 3.35 m/s.

3 Computational model

The flow of the gas in the furnace can be predicted by solving the Navier-Stokes and continuity equations for an incompressible fluid. Due to the high value of Reynolds number, the flow is likely to be strongly turbulent. As a direct numerical simulation of such a flow is practically impossible, due to the need of enormous computing power, modeling is required. Here, the attention is paid to mean flow rather than details of turbulent fluctuations. To model the effect of turbulence on the mean flow, Reynolds Averaged Navier Stokes equations for a turbulent incompressible fluid flow are considered. The mathematical model used to describe the flow field is described in details in Macchion & Zahrai (5). The turbulence quantities are calculated using the Shear Stress Transport (SST) model, see Menter (6). The thermal field is calculated from the numerical integration of the energy equation. The steady state energy equation can be written in an Eulerian reference frame as,

$$\frac{\partial}{\partial x_i}\rho U_i h = \frac{\partial}{\partial x_i}\left(\lambda\frac{\partial T}{\partial x_i} - \rho\overline{u_i h}\right). \qquad (1)$$

where h the enthalpy, x_i is the spatial coordinate, ρ is the fluid mass density, λ is the thermal conductivity of the fluid, and the velocity field is decomposed in an averaged part U_i and a fluctuating part u_i. The quantities U_i and u_i being known from numerical integration of the hydrodynamic and turbulence equations, only the thermal terms in equation 1 remain to be calculated. The term $\overline{u_i h}$ is known as the turbulent heat flux vector, and

at constant heat capacity is proportional to $\overline{u_i T}$ which is modelled.

In analogy to the modelling of the turbulent stress tensor and in the absence of source terms, the temperature equation is written as:

$$C_p \frac{\partial \rho U_i T}{\partial x_i} = \frac{\partial}{\partial x_i}\left[\left(\frac{\mu}{Pr} + \frac{\mu_t}{Pr_t}\right)\frac{\partial T}{\partial x_i}\right] \qquad (2)$$

where μ denotes the dynamic viscosity of the fluid, Pr is the Prandtl number of the fluid. As stated in (7) experiments and analysis place the turbulent Prandtl number Pr_t close to 0.9, and this value is also used in the present formulation. The transport properties were calculated using the Sutherland formula, see (8).

Automatic wall treatment as described in (7) and (9) is used for treatment of solid walls. To solve the system formed by the hydrodynamic, turbulence, and energy equations, a commercially available code, CFX 5.6 is used. The equations are discretized on an unstructured, non-staggered mesh by a finite volume formulation. The continuity equation is approximated using a second order central difference approximation to the first order derivative in velocity, modified by a fourth order derivative in pressure based on the Rhie-Chow interpolation method. The advection scheme used in this study is the high resolution scheme, a form of total variation diminishing scheme, proposed by Barth and Jesperson (10). A coupled solver is used to solve the set of discretized equations. Details of the numerical method used in the code CFX-5 can be found in (9).

4 Results

In this section thermal effects in the two charges are presented. The performance of a furnace can be expressed in terms of total cooling efficiency averaged over all work pieces. The best solution will be the one resulting in homogeneous heat transfer over each work piece with small variations between the pieces.

The mean heat transfer in the present furnace, averaged over all work spieces, $\overline{h}$, was found to be 290 W·m^{-2}·K^{-1} and 330 W·m^{-2}·K^{-1} when the furnace was charged with plates and cylinders, respectively, with RMS values of 0.49 and 0.52 for each case. Minimum and maximum values of the local heat transfer, h_{min} and h_{max}, are lower by 50 % and higher by 500 % of the mean values, respectively. These data are presented in table 1, where also the minimum and maximum values of the local heat transfer, h_{min} and h_{max}, are shown for each case. As found in that table, locally very low and very high values can be obtained.

Configuration	$\overline{h}$	$\overline{Nu}$	h_{rms}	h_{min}	h_{max}
Plates	290	770	0.49	120	1600
Cylinders	330	1480	0.52	70	1150

Table 1: Global heat transfer coefficient and its variations

The mean Nusselt number, defined by

$$\overline{Nu} = \overline{h}D/k,$$

is 770 for plates at a Reynolds number of Re_{plates} = 1.8 · 10^6, and 1480 for cylinders at $Re_{cylinders}$ = 2.3 · 10^6. D in the above formula is 0.07 m for plates and 0.12 m for the cylinders.

Figure 2 presents streamwise velocity, shaded contours on the symmetry plane at z = 0 of the furnace chamber in the case with plates. The uniform flow region previously identified in (5) is clearly visible upstream of the plates, in clear grey colour on the figure. The flow around the plates is featured by the presence of separation bubbles, dark grey region, on the sides of certain plates. The fact that there exists separation bubbles only on some sides of the plates arises from the expanding shape of the incoming flow, and from remaining non-uniformities in the upstream flow. When the separation bubble exists it is about one plate thickness long. Large recirculation flows can be seen behind each of the plates.

Most of the preceding flow features can also be identified on figure 3, which presents streamwise velocity contours on the symmetry plane at z = 0 of the furnace chamber in the case with cylinders. When a separation bubble is formed it is about one cylinder diameter long. The velocity contours around the cylinder $C_{(-1)(-1)(0)}$ show a large recirculation bubble, dark grey region on one side, while high speed fluid flowing downtream and non-recirculating is seen on the other side. Such behaviour can be seen on other parts of the load, for instance on cylinder $C_{(0)(+1)(0)}$. As it will be discussed later, three-dimensionality in the flow field leads to similar character of the thermal field.

Figure 4 presents velocity profiles between and heat transfer coefficient over plates $P_{(0)}$ and $P_{(-1)}$. These two plates were seen to be characteristic of the flow properties within the uniform flow region. Figure 4(b) presents the heat transfer coefficient distribution on plates $P_{(0)}$ and $P_{(-1)}$. The two distributions are fairly similar. Beyond x = 0 the heat transfer coefficient is slightly diminishing. Between x = -0.25 and x = 0 the heat transfer coefficient has a strong variation.

Figure 4(a) shows six velocity profiles at six locations starting from the upstream edges of the plates $P_{(0)}$

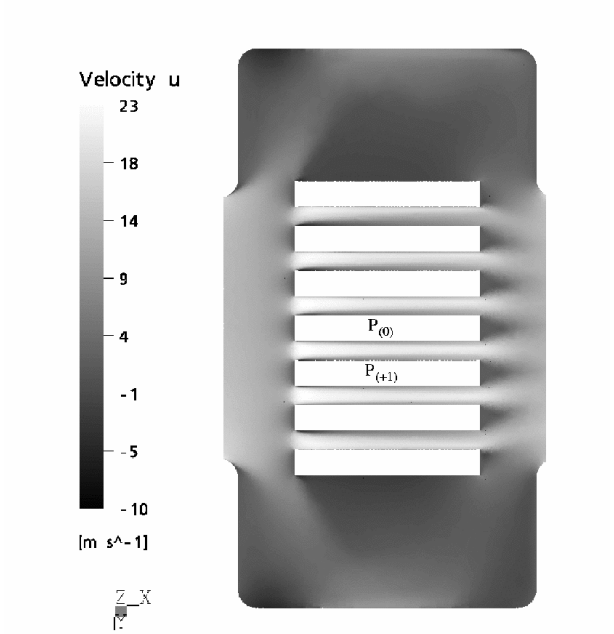

Figure 2: Contours of streamwise velocity U along the symmetry plane of the furnace chamber- Case with plates

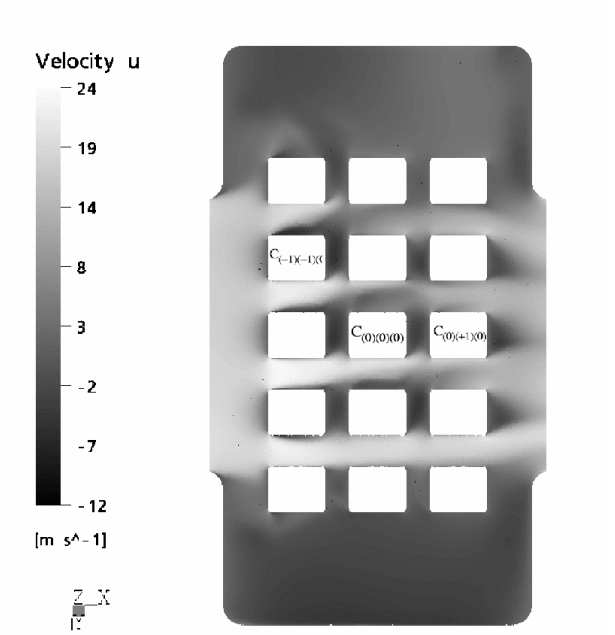

Figure 3: Contours of streamwise velocity U along the symmetry plane of the furnace chamber- Case with cylinders

and $P_{(-1)}$ and ending at their downstream edges. The flow appears to be developing all along the plate and does not reach any well-defined fully developed profile. The velocity profiles at the leading edge, x = -0.25 and at the trailing edge x = 0.25 are alike in shape and differ from the profiles at x = -0.15, x = -0.05, x = 0.05, x = 0.15 which resemble developing flow profiles. No separation bubble is visible on figure 4(a). Careful look at the solution shows that when there is a separation bubble, it is about 7 cm long, which corresponds to the thickness of the plates. Profiles at x = 0.05, x = 0.15 are somewhat flatter than at $x < 0$.

Figure 5 presents some streamwise velocity and heat transfer coefficient profiles over six neighbouring cylinders in the case charged with cylinders. The profiles are based on curves perpendicular to the symmetry plane at z = 0. In figure 5(a) the velocity profiles appear flatter on the four last cylinders, $C_{(0)(0)(0)}$, $C_{(+1)(0)(0)}$, $C_{(+1)(0)(+1)}$, and $C_{(0)(0)(+1)}$ than on the two first cylinders, $C_{(-1)(0)(0)}$ and $C_{(-1)(0)(+1)}$. The velocity profiles on the first set of cylinders at x = -0.28, x = -0.21, and x = -0.14 are not symmetric. They show that the flow is entirely separated on the cylinder $C_{(-1)(0)(0)}$ (Z = 0.06) while the flow is not separated on cylinder $C_{(-1)(0)(+1)}$. It is important to stress that these observations are not valid for the whole circumference of the cylinders. Figure 5(b) shows the heat transfer coefficient to be higher on the first row of cylinders, $C_{(-1)(0)(0)}$ and $C_{(-1)(0)(+1)}$ than on the two following rows.

Figure 6 details the heat transfer coefficient evolution over plates $P_{(0)}$ and $P_{(+3)}$ in the case with plates. Plates $P_{(0)}$ and $P_{(+3)}$ are chosen since they represent two extreme cases; plate $P_{(0)}$ is located in the middle of the charge and plate $P_{(+3)}$ on the side. Consequently, the one in the middle experiences a uniform flow while the one on the side suffers of the slow and recirculating flows in the dead volumes. The mean heat transfer is about twice as large from z = 0.0 to z = 0.15 on plate $P_{(0)}$ than on plate $P_{(+3)}$. Between x = -0.2 and x = 0.2 the heat transfer coefficient on plate $P_{(+3)}$ remains nearly constant at about h_w = 100 W $\cdot$ m^{-2} $\cdot$K^{-1}, while on plate $P_{(0)}$ it is much closer to h_w = 350 W $\cdot$ m^{-2} $\cdot$K^{-1}. The value of h_w is almost constant on plate $P_{(+3)}$ between x = -0.2 and x = 0.0, while on plate $P_{(0)}$ it shows an oscillatory behaviour. The heat transfer coefficient close to the edge of plates $P_{(0)}$ and $P_{(+3)}$, at z = 0.25, are about the same between x = 0.0 and x = 0.25, and slightly higher on plate $P_{(0)}$ than on plate $P_{(+3)}$ between x = -0.25 and x = 0.0. The maximum values of the heat transfer coefficient at the edge of the plate at x = -0.25 is about twice as large on plate $P_{(0)}$ as on plate $P_{(+3)}$.

Figure 7 presents the heat transfer coefficient distri-

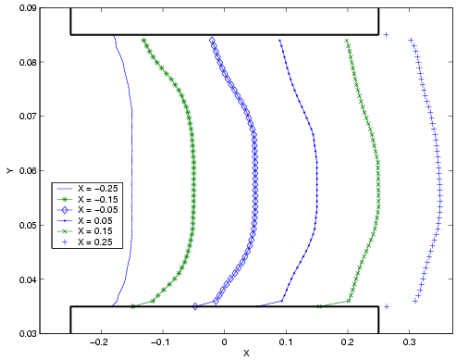

(a) Velocity profiles between plates $P_{(0)}$ and $P_{(-1)}$

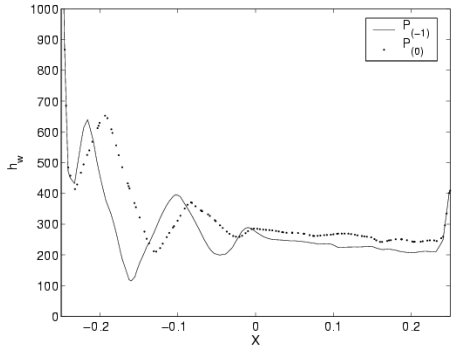

(b) Heat transfer coefficient distribution on plates $P_{(0)}$ and $P_{(-1)}$

Figure 4: Relation between velocity profile and heat transfer coefficient evolution in the uniform flow region - case with plates

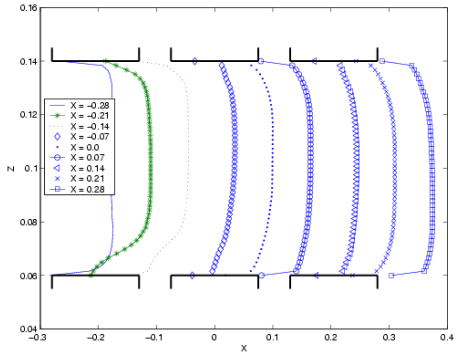

(a) Velocity profiles between cylinders $C_{(-1)(0)(0)}$ and $C_{(-1)(0)(+1)}$, $C_{(0)(0)(0)}$ and $C_{(0)(0)(+1)}$,$C_{(+1)(0)(0)}$ and $C_{(+1)(0)(+1)}$,

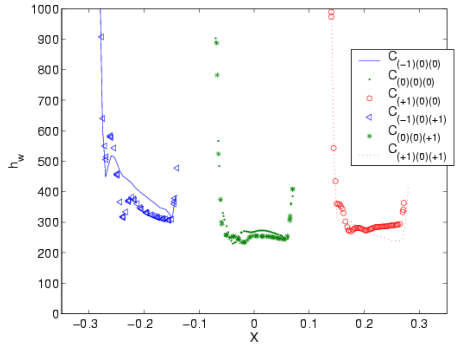

(b) Heat transfer coefficient distribution on cylinders $C_{(-1)(0)(0)}$ and $C_{(-1)(0)(+1)}$, $C_{(0)(0)(0)}$ and $C_{(0)(0)(+1)}$,$C_{(+1)(0)(0)}$ and $C_{(+1)(0)(+1)}$

Figure 5: Relation between velocity profile and heat transfer coefficient evolution in the uniform flow region - Case with cylinders

bution around the half-cylinder $C_{(0)(0)(0)}$, situated in the middle of the charge and on the symmetry plane of the furnace chamber. The heat transfer coefficient is given along six curves parallel to the axis of the cylinder and at different angles θ spanning the whole circumference of the cylinder, from θ = 5^o to θ = 175^o. No clear pattern can be found in the way the heat transfer coefficient varies over the surface of the cylinder. The heat transfer coefficient is higher close to the leading and trailing edges. The heat transfer coefficient distribution is fully three-dimensional, as it can be seen that the cooling is more efficient at θ = 45^o and θ = 175^o.

5 Conclusion

In this work, thermal effects in a gas quenching furnace have been investigated by means of numerical simulations. A quenching load appears to be a very complex thermal body subjected to extremely large variations in heat transfer. These variations arise primarily from the design of the quenching chamber. The load being partly in the high velocity region, partly in the low velocity region, experiences large variations in the heat transfer coefficient from the load edge to the load center. As already pointed out in Macchion et al (5) it appears that the design of the quenching chamber should focus on getting rid of geometrical features generating complex flow. An example of such improvements would consist in adapting the width of the working chamber to the width of the load to be quenched.

The present study shows also that the thermal field is particularly sensitive to piece position through the charge, the bodies being placed in the central position

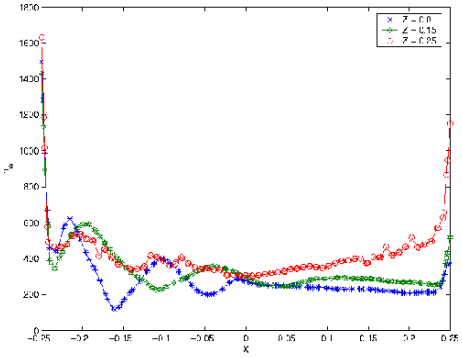

(a) Plate $P_{(0)}$

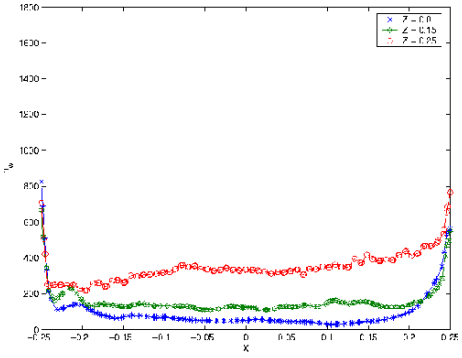

(b) Plate $P_{(+3)}$

Figure 6: Heat transfer coefficient distribution over the plates - Case with plates

exhibiting more uniform heat transfer distributions. This work, accompanied by others such as the study performed by Wiberg (11), shows also that the separated flow over a bluff cylinder in axial flow leads also to variations in the Nusselt number up to 125 %.

As a result the heat transfer non uniformity is the interaction of three geometrical parameters: (1) geometry of the quenching chamber, (2) charge configuration, (3) load parts shape. As such it would seem reasonable to propose either guiding devices within the charge to limit the influence of neighbouring bodies, either to use only the central area of the quenching chamber for quenching.

6 Acknoledgements

This work was carried out at the Royal Institute of Technology, Stockholm, with the financial support of Ipsen International GmbH, and Linde Gas GmbH.

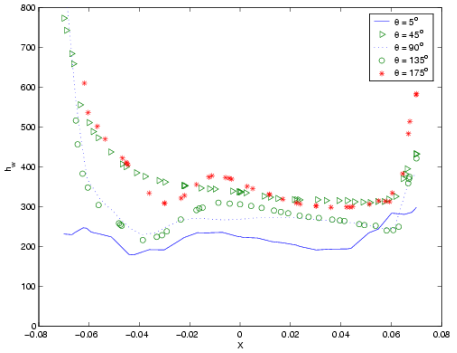

Figure 7: Heat transfer coefficient over the cylinder $C_{(0)(0)(+1)}$- Case with cylinders

References

[1] E. Troell, S. Segerberg, Kylning i kvve och helium under hgt tryck (cooling in nitrogen and helium under high pressure), Tech. Rep. IVF-Skrift 95845, The Swedish Institute of Production Engineering Research (IVF), Gteborg (1995).

[2] A. Thuvander, A. Melander, M. Lind, N. Lior, F. Bark, Prediction of convective heat transfer coefficients and examination of their effects on distortion of tubes quenched by gas cooling, in: 4th ASM Heat Treatment and Surface Eng. Conf. in Europe, Florence, Italy, 1998.

[3] F. Bless, B. Edenhofer, Advances in increasing the quenching speed of single-chamber vacuum furnaces with high-pressure gas-quench systems, Heat Treatment of Metals 1997.4 (1997) 89–91.

[4] J. E. Pritchard, G. Nurnberg, M. Shoukri, Computer modelling of pressure gas quenching in vacuum furnaces, Heat Treatment of Metals 1996.4 (1996) 79–83.

[5] O. Macchion, S. Zahrai, J. Bouwman, On hydrodynamics of gas quenching furnace, Submitted to the Journal of Materials Processing Technology.

[6] F. Menter, Zonal two equation k-ω turbulence models for aerodynamic flows, AIAA Paper 93-290624th Fluid Dynamics Conference (Orlando).

[7] W. Vieser, T. Esch, F. Menter, Heat transfer predictions using advanced two-equation turbulence models, Tech. Rep. CFX-VAL10/0602, CFX (June 2001).

[8] C. Molina, O. Macchion, Gas composition influence on transport properties and heat transfer

within the frame of gas quenching applications, Tech. rep., KTH Mekanik, Stockholm (September 2004).

[9] ANSYS, ANSYS CFX Reference Manual, cfx-support-uk@ansys.com (February 2004).

[10] T. Barth, D. Jesperson, The design and application of upwind schemes on unstructured meshes, AIAA Paper 89-0366.

[11] R. Wiberg, N. Lior, Convection heat transfer coefficients for axial flow gas quenching of a cylinder, in: Proceedings of the Fourth International Conference on Quenching and the Control of Distortion, 2003.